

Switchable multi-wavelength Tm-doped mode-locked fiber laser

Zhiyu Yan,^{1,2} Yulong Tang,¹ Biao Sun,^{1,2} Tao Liu,¹ Xiaohui Li,¹ Perry Shum Ping,^{1,3} Xia Yu,^{2,4} Ying Zhang,² and Qi Jie Wang^{1,3,5}

¹OPTIMUS, Photonics Center of Excellence, School of Electrical and Electronic Engineering, Nanyang Technological University, 50 Nanyang Ave, 639798, Singapore

²Precision Measurements Group, Singapore Institute of Manufacturing Technology, 71 Nanyang Drive, 638075, Singapore

³COFT, Centre for Optical Fiber Technology, Nanyang Technological University, 637371, Singapore

⁴e-mail: xyu@simtech.a-star.edu.sg

⁵e-mail: qjwang@ntu.edu.sg

Received February 3, 2015; revised March 28, 2015; accepted March 29, 2015;
posted March 31, 2015 (Doc. ID 233654); published April 20, 2015

We propose and demonstrate for the first time a switchable tri-wavelength Tm-doped ultra-fast fiber laser based on nonlinear polarization evolution (NPE) technique. The NPE effect induces wavelength-dependent loss in the cavity that changes the homogeneous broadening of the effective gain to become inhomogeneous. This inhomogeneous effective gain spectral profile enables the multi-wavelength mode locking. Binary control of three bits can be realized by controlling the polarization in the compact fiber ring cavity. Such switchable laser has potential applications in optical signal processing and communication. © 2015 Optical Society of America

OCIS codes: (140.3510) Lasers, fiber; (140.4050) Mode-locked lasers.

<http://dx.doi.org/10.1364/OL.40.001916>

Multi-wavelength fiber laser can be widely used in optical sensing, precision spectroscopy, and wavelength division multiplexing communication [1]. For continuous wave (CW) operation, Tran *et al.* realized switchable four-wavelength lasing in an erbium-doped fiber laser by the nonlinear optical loop mirror technique incorporating multiple fiber Bragg gratings [2]. Zhang *et al.* and Feng *et al.* realized more than 20-wavelength CW lasing in an erbium-doped fiber laser with the birefringent fiber filtering and nonlinear polarization evolution (NPE), respectively [3,4]. Multi-wavelength lasing could also be realized by adding a long single-mode fiber (SMF) or photonic crystal fiber in the laser cavity to induce four-wave mixing effect [5,6]. Up to 42-wavelength lasing was realized in a CW thulium-doped fiber laser by nonlinear amplifier loop mirror [7]. For multi-wavelength operation in the pulsed regime, optical components such as active modulator and saturable absorber were required to be integrated in the cavity, which increased the complexity and overall loss of the system [8–12]. In the 1- μm and 1.5- μm wavelength regime, tri-wavelength and five-wavelength pulsed lasing have been reported [13,14]. While in the 2- μm regime, only dual-wavelength pulsed lasing was reported so far, which was achieved by adjusting the polarization controllers [15].

In this Letter, tri-wavelength mode locking with full binary control is experimentally demonstrated in a Tm-doped fiber laser for the first time by using the NPE technique. This is of much interest as it could act as an optical binary system, which has potential applications in optical signal processing, optical switching devices, and optical communication. In the experiment, the NPE technique is used not only for mode-locked operation, but also for inducing wavelength-dependent loss (i.e., tuning the cavity transmission) to enable the multi-wavelength lasing in a compact setup.

The configuration of the proposed fiber laser is shown in Fig. 1. The gain medium is a 1.5-m Tm-doped fiber

(Nufern, core/cladding diameter: 9/125 μm , NA: 0.15, core absorption: 27 dB/m at 793 nm), which is bidirectionally pumped by two 793-nm laser diodes (LD) with maximum output power of 170 mW and 200 mW, respectively. The pump light from one LD is coupled into the cavity by a wavelength-division multiplexer (WDM), and the pump light from the other LD is launched into the cavity by a 2×2 coupler with a 40:60 splitting ratio. The coupler also serves for light output coupling. With this coupler, 40% of the $\sim 2000\text{-nm}$ light will continue to circulate inside the cavity, and 60% will be output. A 70-m silica SMF is used as the birefringent fiber. With 1-m fiber pigtail in the coupler, WDM and polarization-dependent isolator (PD-ISO), the total cavity length is around 77.5-m. The output is connected to an optical spectrum analyzer and a 33-GHz oscilloscope together with a 7-GHz photo-detector to simultaneously measure the spectra and the pulse train.

Mode locking of the fiber laser is achieved by the NPE principle. The output pulses are solitons with the typical Kelly sidebands [16]. Stable tri-wavelength mode locking at the wavelength of 1863/1874/1886 nm is obtained when tuning the PCs and increasing the pump power to

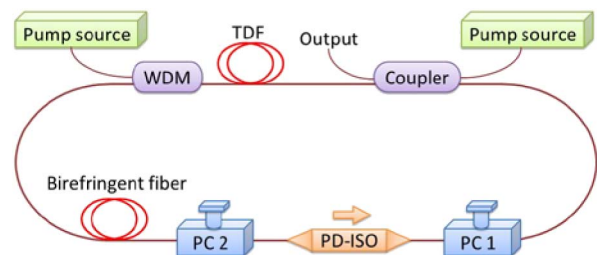


Fig. 1. Experimental setup of the proposed multi-wavelength mode-locked Tm-doped fiber laser using nonlinear polarization evolution technique. PC, polarization controller; PD-ISO, polarization-dependent isolator; WDM, wavelength-division multiplexer; TDF, Tm-doped fiber.

350 mW. The separation of two adjacent wavelengths is around 11 nm. Interestingly, the tri-wavelength operation can be switched either one-by-one or pair-by-pair, which is able to cover the full binary range, as shown in Fig. 2. For the pair-by-pair switchable operation, the pair of 1863/1886 nm does not appear. The first peak at the wavelength of 1861 nm is a CW laser emission instead of the expected soliton mode at 1863 nm. This indicates the coexistence of CW light and soliton pulses in the cavity.

The 3-dB bandwidth of the soliton with the center wavelength of 1863 nm is measured to be 3.5 nm, as shown in Fig. 3(a). The autocorrelation measurement shows a pulse width of 3.11 ps as illustrated in Fig. 3(b). The time-bandwidth product is 0.944, indicating that the intra-cavity pulses are chirped. In the stable tri-wavelength regime, the oscilloscope trace in Fig. 3(d) clearly shows that three soliton pulses coexist in the cavity. The perfect alignment with single-wavelength pulse train in Fig. 3(c) eliminates the possibility of pulse-splitting. The repetition rate of 2.68 MHz corresponds to the cavity round-trip frequency. The output laser beam shows a symmetric Gaussian profile, as shown in Fig. 3(e), and the beam quality is guaranteed by the adopted single-mode fiber. The maximum output power achieved is 3 mW. It is mainly due to the insertion losses of the coupler and isolator, as well as the transmission loss of the 77.5-m SMF at this operating wavelength.

Besides the tri-wavelength mode locking, we also observe mode locking in multi-soliton state, single-scale state, tunable single-wavelength emission, and tunable and switchable dual-wavelength emission when the power or the setting of PCs is changed. Some factors

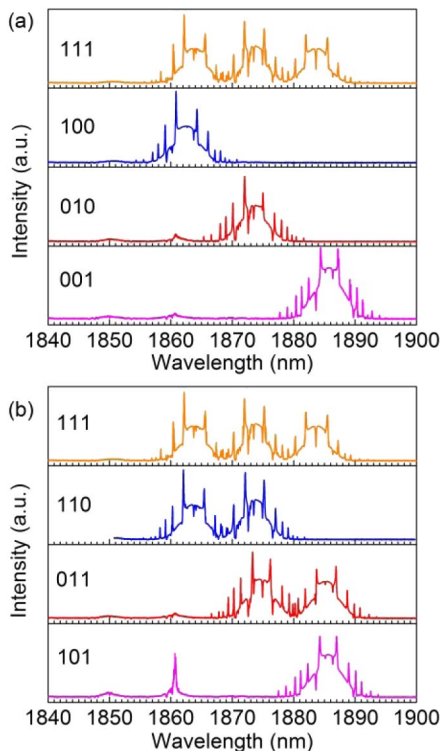


Fig. 2. Switchable tri-wavelength mode locking at the wavelength of 1863/1874/1886 nm with (a) one-by-one and (b) pair-by-pair appears at each time.

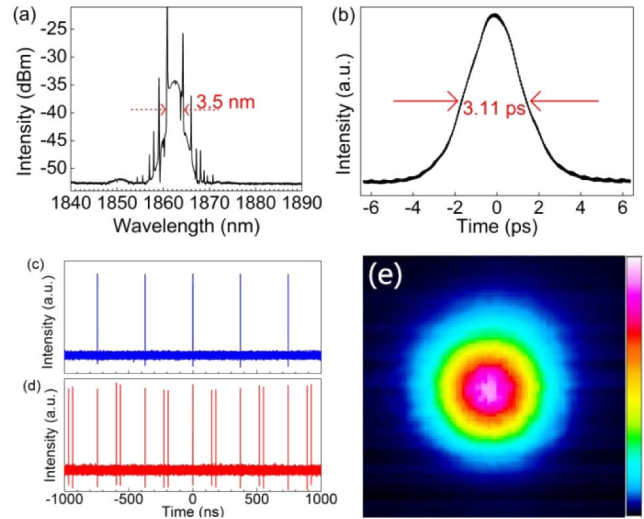


Fig. 3. (a) Spectrum and (b) pulse width of one soliton with center wavelength at 1863 nm. (c) Single-wavelength and (d) tri-wavelength pulse train of the mode-locked fiber laser. (e) The beam profile.

such as NPE, long cavity, and soliton collapse are responsible for it [17–20]. The tri-wavelength mode locking is repeatable by two-step adjustment of PCs. The first step is coarse adjustment of the PCs to get the stable tri-wavelength mode locking. The second step is fine adjustment of the PCs around that position to get the switchable operation.

For the PD-ISO, the two PCs and the birefringent fiber can change the cavity transmission [19] as follows:

$$T = \cos^2 \theta_1 \cos^2 \theta_2 + \sin^2 \theta_1 \sin^2 \theta_2 + \frac{1}{2} \sin(2\theta_1) \sin(2\theta_2) \cos(\Delta\varphi_L + \Delta\varphi_{NL}). \quad (1)$$

The cavity transmission is changed when the polarization states of PCs change (i.e., θ_1 , θ_2 , and B_m). Our calculation shows that the modulation depth can be more than 80%, which strongly depends on the value of θ_1 and θ_2 . The period of modulation mainly depends on the linear cavity phase delay $\Delta\varphi_L$ because the nonlinear cavity phase delay $\Delta\varphi_{NL}$ is much smaller than it. We consider $\Delta\varphi_L$ in the simulation. The description and the value of parameters used are listed in Table 1.

The periodic modulation of cavity transmission will induce the periodic modulation of effective gain (net gain minus cavity loss) profile in the whole cavity, resulting in the inhomogeneous effective gain profile in the cavity. This induces the multi-wavelength mode-locked lasing.

The laser emits at the wavelength with the maximum effective gain due to gain competition. Therefore, for the single-wavelength emission of a laser without modulating the cavity transmission, only one-period effective gain spectrum exists with one peak wavelength. In order to achieve the multi-wavelength laser operation, multi-period effective gain spectrum should be designed. Since the effective gain profile is modulated by the cavity transmission, the cavity transmission should be periodically modulated. The one-period wavelength separation $\Delta\lambda$ should be small so as to have multiple peaks in the

Table 1. List of Parameters Used in the Simulation

	Description	Value
θ_1	Angle between the fast axes of the birefringent fiber and the polarization direction	$\pi/5$
θ_2	Angle between the fast axes of the birefringent fiber and the orientation of polarizer	$\pi/4.5$
$\Delta\varphi_L$	Linear cavity phase delay	$2\pi LB_m/\lambda$
L	Birefringent fiber length	70 m
B_m	Modal birefringence	4.94×10^{-6}

effective gain spectrum. The working principle can be clarified as follows:

According to Eq. (1), the cavity transmission reaches the maximum when $\Delta\varphi_L + \Delta\varphi_{NL} \approx \Delta\varphi_L = 2\pi N$, N is an integer which is expressed as

$$N = LB_m/\lambda. \quad (2)$$

The wavelength separation $\Delta\lambda$ of one period is expressed as

$$LB_m \left(\frac{1}{\lambda} - \frac{1}{\lambda + \Delta\lambda} \right) = 1. \quad (3)$$

Theoretically, a large L is necessary in order to generate multiple peaks within a limited gain bandwidth, subjected to the constraint that B_m can be tuned over a small range only. However, if the cavity length is too long in a passively mode-locked fiber laser system, the stability of the pulsed laser output will be negatively affected.

The simulation result of the cavity transmission is shown in Fig. 4(a). The separation of adjacent peaks is around 11 nm, which matches our experimental results in Fig. 4(b).

By tuning the PCs, the θ_1 , θ_2 , and B_m will be changed. θ_1 and θ_2 will affect the modulation depth of the cavity transmission, θ_1 , θ_2 , and B_m will affect the position of maximum points of cavity transmission. The effective gain profile will be changed when any of the above factors changes. Therefore one-by-one, pair-by-pair, and tri-wavelength lasing appear under different operation conditions with different effective gain profiles.

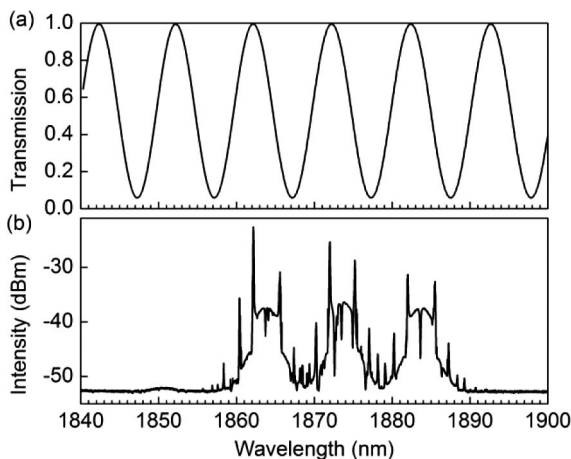


Fig. 4. Comparison between (a) the simulation and (b) the experimental results. The separation between each peak is ~ 11 nm in both simulation and experimental results.

According to Eq. (3), once the cavity length is determined, the separation of two lasing peaks $\Delta\lambda$ can be changed a little. In order to get simultaneous soliton emission at both 1863 and 1886 nm, which is shown in Fig. 2(b), the separation of two wavelengths has to change from 11 to 23 nm. This requires B_m to be changed largely, which is not easy to realize. Thus we only observe one CW lasing and one soliton emission in this case.

Theoretically, we can obtain more than tri-wavelength lasing. The lasing emission at each wavelength is sensitive to the polarization states, the gain and the loss. Hence, further precise electronic control of the polarization state will potentially enable more lasing peaks.

In conclusion we have demonstrated for the first time the switchable tri-wavelength mode locking in a Tm-doped fiber laser based on the NPE technique. The multi-wavelength and switchable operation results from the wavelength-dependent loss of the cavity induced by the NPE effect. Soliton emission in both formats of one-by-one and pair-by-pair switching has been experimentally obtained. 3-bits binary operation of mode-locking has been realized by simply changing the polarization states. The experimental observations have been verified by numerical calculation. This provides a simple and compact solution to achieve multi-wavelength emission and switchable mode locking in fiber lasers.

The authors thank Ms. Yanyan ZHOU and Ms. Jiaqi LUO for useful discussions and experimental help, Prof. Dingyuan TANG and Mr. Guodong SHAO for equipment support. We would like to acknowledge financial support from A*STAR SERC Innovation in Remanufacturing Programme (Grant No. 112 290 4018) and A*STAR SERC Advanced Optics in Engineering Programme (Grant No. 122 360 0004).

References

1. X. Li, Y. Wang, Y. Wang, X. Hu, W. Zhao, X. Liu, J. Yu, C. Gao, W. Zhang, Z. Yang, C. Li, and D. Shen, *IEEE Photon. J.* **4**, 234 (2012).
2. T. V. A. Tran, K. Lee, S. B. Lee, and Y. Han, *Opt. Express* **16**, 1460 (2008).
3. Z. Zhang, L. Zhan, K. Xu, J. Wu, Y. Xia, and J. Lin, *Opt. Lett.* **33**, 324 (2008).
4. X. Feng, H. Tam, and P. K. A. Wai, *Opt. Express* **14**, 8205 (2006).
5. Y.-G. Han, T. V. A. Tran, and S. B. Lee, *Opt. Lett.* **31**, 697 (2006).
6. H. B. Sun, X. M. Liu, L. R. Wang, X. H. Li, and D. Mao, *Laser Phys.* **20**, 1994 (2010).
7. W. Peng, F. Yan, Q. Li, S. Liu, T. Feng, and S. Tan, *Laser Phys. Lett.* **10**, 115102 (2013).
8. Z. Luo, A. Luo, W. Xu, H. Yin, J. Liu, Q. Ye, and Z. Fang, *IEEE Photon. J.* **2**, 571 (2010).

9. X. Wang, Y. Zhu, P. Zhou, X. Wang, H. Xiao, and L. Si, *Opt. Express* **21**, 25977 (2013).
10. S. Pan and C. Lou, *IEEE Photon. Technol. Lett.* **18**, 1451 (2006).
11. H. Zhang, D. Y. Tang, X. Wu, and L. M. Zhao, *Opt. Express* **17**, 12692 (2009).
12. Y. S. Fedotov, S. M. Koltsev, R. N. Arif, A. G. Rozhin, C. Mou, and S. K. Turitsyn, *Opt. Express* **20**, 17797 (2012).
13. S. Huang, Y. Wang, P. Yan, J. Zhao, H. Li, and R. Lin, *Opt. Express* **22**, 11417 (2014).
14. Z. W. Xu and Z. X. Zhang, *Laser Phys. Lett.* **10**, 085105 (2013).
15. A. Y. Chamorovskiy, A. V. Marakulin, A. S. Kurkov, and O. G. Okhotnikov, *Laser Phys. Lett.* **9**, 602 (2012).
16. S. M. J. Kelly, *Electron. Lett.* **28**, 806 (1992).
17. S. Koltsev, S. Smirnov, S. Kukarin, and S. Turitsyn, *Opt. Fiber Technol.* **20**, 615 (2014).
18. S. Smirnov, S. Koltsev, S. Kukarin, and A. Ivanenko, *Opt. Express* **20**, 27447 (2012).
19. D. Y. Tang, L. M. Zhao, B. Zhao, and A. Q. Liu, *Phys. Rev. A* **72**, 043816 (2005).
20. Z. Yan, X. Li, Y. Tang, P. P. Shum, X. Yu, Y. Zhang, and Q. J. Wang, *Opt. Express* **23**, 4369 (2015).